

Stress Distribution in Functionally Graded Nanocomposite Cylinders Reinforced by Wavy Carbon Nanotube

R. Moradi-Dastjerdi*

Young Researchers and Elite Club,
Khomeinishahr Branch, Islamic Azad University, Khomeinishahr, Iran
E-mail: rasoul.moradi@iaukhsh.ac.ir

*Corresponding author

M. M. Sheikhi & H. R. Shamsolhoseinian

School of Mechanical Engineering, Shahid Rajaei Teacher Training
University (SRTTU), Tehran, Iran
E-mail: m.sheikhi@srttu.edu

Received: 6 June 2014, Revised: 24 October 2014, Accepted: 19 November 2014

Abstract: This work mainly reports effects of aspect ratio and waviness index of carbon nanotubes on the stress and displacement distributions of functionally graded nanocomposite cylinders reinforced by wavy single-walled carbon nanotubes based on mesh-free method. In this simulation, an axisymmetric model is used and three linear types of functionally graded distributions of wavy CNTs along the radial direction of cylinder are considered, and their results are compared with results of a uniform distribution. The material properties are estimated by a micro mechanical model. In the mesh-free analysis, moving least squares shape functions are used for approximation of displacement field in the weak form of motion equation and the transformation method was used for imposition of essential boundary conditions. Also, the effects of volume fraction and distribution pattern of wavy CNTs and cylinder thickness are investigated on the static responses of carbon nanotube reinforced composite cylinders subjected to internal or external pressure. It is observed that waviness has a significant effect on the effective reinforcement of the nanocomposites.

Keywords: Aspect Ratio, Mesh-Free, Nanocomposite Cylinder, Stress Distribution, Wavy Carbon Nanotube

Reference: Moradi Dastjerdi, R., Sheikhi, M. M., and Shamsolhoseinian, H. R., "Stress Distribution in Functionally Graded Nanocomposite Cylinders Reinforced by Wavy Carbon Nanotube", Int J of Advanced Design and Manufacturing Technology, Vol. 7/ No. 4, 2014, pp. 43-54.

Biographical notes: **R. Moradi-Dastjerdi** is a member of Young Researchers and Elite Club of Islamic Azad University Khomeinishahr Branch since 2010. He is currently PhD student in Mechanical Engineering of Shahid Rajaei Teacher Training University (SRTTU), Tehran, Iran. His research interests include Solid Mechanics, Mechanics of Composite Materials, Nanocomposites, and Mesh-free. **M. M. Sheikhi** received his PhD in Mechanical Engineering from University of Tarbiat Modares, Tehran, Iran in 2008. **H. R. Shamsolhoseinian** received his MSc in Mechanical Engineering from Shahid Rajaei Teacher Training University (SRTTU), Tehran, Iran in 2014.

1 INTRODUCTION

After carbon nanotube (CNT) discovery by Iijima, CNTs have attracted much attention from researchers. Owing to their remarkable mechanical, electrical and thermal properties, CNTs have been widely accepted as a potential constituent of reinforcement and multi-functional element for nanocomposites [1]. Most investigations of carbon nanotubes reinforced composites (CNTRCs) have focused on material properties where researchers have discovered that mechanical, electrical and thermal properties of polymer composites can be considerably improved by adding small amounts of CNTs [2-5]. Gojny et al., focused on the evaluation of different types of CNTs applied, their influence on the mechanical properties of epoxy-based nanocomposites and the relevance of surface fictionalization [6]. Combination of the previously mentioned material properties makes CNTs highly desirable candidates to improve the properties of polymers.

Fidelus et al., investigated thermo-mechanical properties of epoxy-based nanocomposites based on low weight fraction of randomly oriented single- and multi-walled CNTs [7]. Han and Elliott determined the elastic modulus of composite structures under CNTs reinforcement by molecular dynamic (MD) simulation and investigated the effect of volume fraction of single walled carbon nanotubes on mechanical properties of nanocomposites [8]. Coto et al., employed MD method to show the effect of carboxylic groups attached on the surface of single walled carbon nanotubes (SWCNT) and multi-walled carbon nanotubes (MWCNT) on their Young's modulus and Poisson's ratio along the axial direction of the CNTs [9]. Manchado et al., blended small amounts of arc-SWNT in isotactic polypropylene and observed the modulus increase from 0.85 GPa to 1.19 GPa at 0.75 wt.%. In addition the strength increased from 31 MPa to 36 MPa by 0.5 wt.%. Both properties were observed to fall off at higher loading levels [3].

Also Qian et al., [4] have shown that with only 1% (by weight) of CNTs added in a matrix material, the stiffness of a resulting composite film can increase between 36 and 42% and the tensile strength by 25%, which indicates significant loading transfer across the nanotube-matrix interface. Functionally graded materials (FGMs) are inhomogeneous composite materials with gradient compositional variation of the constituents (e.g., metal and ceramic) from one surface of the material to the other, which results in continuously varying material properties. The materials are intentionally designed in such a way that they possess desirable properties for specific applications. Also, as mentioned before, the use of CNT

reinforcement is a focal point in the design of polymer structures. On the other hand, due to high cost of CNTs, it is important to assure that a given amount of reinforcement is optimally used (distributed) in the polymer specimens. The composites, which are reinforced by CNTs with grading distribution, are called functionally graded carbon nanotube reinforced composites (FG-CNTRCs). Therefore, using the concept of FGM can lead to this aim.

Shen [10-11] suggested that the interfacial bonding strength can be improved through the use of a graded distribution of CNTs in the matrix and examined nonlinear bending behavior of simply supported, functionally graded nanocomposite plates reinforced by single walled carbon nanotubes subjected to a transverse uniform or sinusoidal loading in thermal environment. He also investigated post-buckling of nanocomposite cylindrical shells reinforced by SWCNTs subjected to axial compression in thermal environment and showed that the linear functionally graded reinforcements can increase the buckling load. Shen and Xiang [12] investigated the large amplitude vibration behavior of FG-CNTRC cylindrical shells in thermal environments. They assumed material properties of CNTRCs are temperature-dependent and solved the motion equations by an improved perturbation technique to determine the nonlinear frequencies of the CNTRC shells.

Montazeri et al. [13] showed that modified Halpin-Tsai equation with exponential aspect ratio can be used to model the experimental result of MWCNTs composite samples. They also demonstrated that reduction in aspect ratio and nanotube length cause a decrease in aggregation and above 1.5 wt.%, nanotubes agglomerate causing a reduction in Young's modulus values. Thus, it is important to determine the effective aspect ratio and arrangement of CNTs on the effective properties of CNTRC. The reinforcement effect of CNTs with different aspect ratio in an epoxy matrix has been carried out by Martone et al., [14]. They showed that progressive reduction of the tubes effective aspect ratio occurs because of the increasing connectedness between tubes upon an increase of their concentration. Also they investigated on the effect of nanotube curvature on the average contacts number between tubes by means of the waviness that accounts for the deviation from the straight particles assumption.

In two near works, the effects of waviness and aspect ratio of nanotube on the vibrational behavior of CNT-reinforced cylinders are considered [15-16]. They used a new version of rule of mixture to show the effect of waviness of CNT on the vibrational behavior of nanocomposite cylindrical panel. They considered different waviness conditions with variable aspect ratio and they understood that waviness have a significant effect on the natural frequency of nanocomposite

cylindrical panel. In this paper a mesh-free method is applied for static analysis of FG-CNTRC cylinders. MLS shape functions are used for approximation of displacement field in the weak form of equilibrium equation, like Element-Free Galerkin (EFG), but the transformation method is used for the imposition of essential boundary conditions. In the transformation method, after correction of mesh-free shape functions, essential boundary conditions are imposed as in the FEM. In this method, number of degrees of freedom does not increase unlike EFG. Moradi-Dastjerdi et al., presented static and dynamic analysis of functionally graded nanocomposite cylinders reinforced by straight SWCNTs based on the same mesh-free method that is used in this paper [17-18]. In a near work with [18], elastic wave propagation of finite length FG-CNTRC cylinders was carried out by a mesh-free method based on Radial bases functions [19].

In all the above mentioned works, it is noticed that CNTs are assumed straight, but the effects of CNT waviness and aspect ratio aren't considered. In practice, CNT curvature (waviness index) and aspect ratio have important influence on mechanical properties and behaviors. Also static, free vibration, dynamic and stress wave propagation analysis of isotropic FGM cylinders under an impact load were carried out by this mesh-free method [20-22].

In this study, static analysis of nanocomposite cylinders reinforced by wavy SWCNTs is carried out by the mentioned mesh-free method. Four types of distributions of the CNTs are considered; uniform and three kinds of FG distributions along the radial direction of cylinder. Material properties are estimated by a micro mechanical model. Micromechanics equations cannot capture the scale difference between the nano and micro levels. In order to overcome this difficulty, the efficiency parameter is defined and estimated by matching the Young's moduli of CNTRCs obtained by the extended rule of mixture to those obtained by MD simulation like as the applied method in Refs. [15-16]. Effects of CNT waviness and aspect ratio, kind of distribution and volume fraction of carbon nanotubes and also boundary conditions and thickness of cylinder are investigated on the static responses of uniformly distributed (UD) and FG-CNTRC cylinders.

2 MATERIAL PROPERTIES IN FUNCTIONALLY GRADED CNTRC CYLINDERS

Considering a CNTRC cylinder with inner radius r_i , outer radius r_o , where this CNTRC cylinder is made from a mixture of wavy SWCNT (along the radial direction) and an isotropic matrix. The wavy SWCNT

reinforcement is either uniformly distributed or functionally graded in the radial direction. This section discusses the results in the literature on mechanical properties of polymer nanotube composites. A new rule of mixture equation assumes that the fibres are wavy and uniform dispersion of the fibre in the polymer matrix. Also it can't consider the length of fibre therefore it can be modified by incorporating efficiency parameter (η^*) to account for the aspect ratio (AR) and waviness (w) of nanotube [14]. The effective mechanical properties of the CNTRC cylinders are obtained based on a micromechanical model according to [10]:

$$E_1 = \eta_1 V_{CN} E_{1,\eta^*} + V_m E^m \tag{1}$$

$$\frac{\eta_2}{E_2} = \frac{V_{CN}}{E_{2,\eta^*}} + \frac{V_m}{E^m} \tag{2}$$

$$\frac{\eta_3}{G_{12}} = \frac{V_{CN}}{G_{12,\eta^*}} + \frac{V_m}{G^m} \tag{3}$$

$$\nu_{ij} = V_{CN} \nu_{ij}^{CN} + V_m \nu^m \quad i, j = 1,2,3 \text{ and } i \neq j \tag{4}$$

$$\rho = V_{CN} \rho^{CN} + V_m \rho^m \tag{5}$$

Where:

$$E_{i,\eta^*} = \eta^* E_i^{CN} \tag{6}$$

$$\eta^* = 1 - \frac{\tanh(K \cdot AR / (1 + \langle c \rangle))}{K \cdot AR / (1 + \langle c \rangle)} \tag{7}$$

$$K = \sqrt{\frac{-2}{1 + \nu_m} \left/ \left(\frac{E^{CN}}{E^m} \ln(V_{CN}) \right) \right.}$$

where E_i^{CN} , G_{12}^{CN} , ν^{CN} , E_{η^*} , $\langle c \rangle$ and ρ^{CN} are elasticity modulus, shear modulus, Poisson's ratio, effective reinforcement modulus, the average number of contacts per particle and density, respectively, of the carbon nanotube, and E^m , G^m , ν^m and ρ^m are corresponding properties for the matrix. V_{CN} and V_m are the fiber (CNT) and matrix volume fractions and are related by $V_{CN} + V_m = 1$. η_j ($j = 1,2,3$) are the CNT efficiency parameters and they can be computed by matching the elastic modulus of CNTRCs observed from the molecular dynamic (MD) simulation result with the numerical results obtained from the new Rule of mixture in Eqs. (1)-(5). It must be noticed that the average number of contacts, $\langle c \rangle$, for tubes is dependent on their aspect ratio [14]:

$$\langle c \rangle = w \cdot V_{CN} \cdot \left(4 + \frac{3AR^2}{3AR + 2} \right) \tag{8}$$

Where the waviness, w , has been introduced in order to account for the carbon nanotubes curvature within the real composite. According to the literature [14], variation of the excluded volume due to nanotubes curvature has been accounted for by introducing the waviness parameter, w , where the accuracy of this method will be shown by comparison with available literature data.

The profile of the variation of the fiber volume fraction has important effects on the cylinder behavior. In this paper three linear types (FG-V, FG- Λ and FG-X) are assumed for the distribution of CNT reinforcements along the radial direction in FG-CNTRC cylinder. An UD-CNTRC cylinder with the same thickness, referred to as UD, is also considered as a comparator. These distributions along the radial direction are presented as follows (see Fig. 1) [17]:

For type V: $V_{CN} = 2\left(\frac{r-r_i}{r_o-r_i}\right)V_{CN}^*$ (9)

For type Λ : $V_{CN} = 2\left(\frac{r_o-r}{r_o-r_i}\right)V_{CN}^*$ (10)

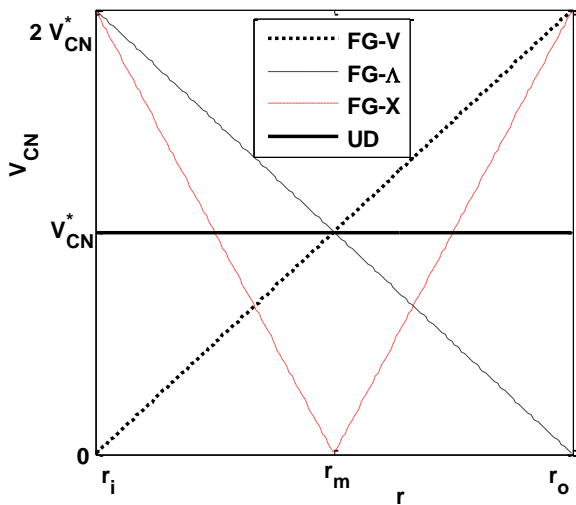


Fig. 1 Variation of nanotube volume fraction (V_{CN}) along the radial direction for types FG-V, FG- Λ , FG-X and UD.

For type X:

$$V_{CN} = 4\left|\frac{r-r_m}{r_o-r_i}\right|V_{CN}^*, \quad r_m = \frac{r_i+r_o}{2}$$
 (11)

For UD: $V_{CN} = V_{CN}^*$ (12)

Where

$$V_{CN}^* = \frac{\rho^m}{\rho^m + (\rho^{CN}/w^{CN}) - \rho^{CN}}$$
 (13)

w^{CN} is the mass fraction of nanotube.

3 GOVERNING EQUATIONS

The weak form of equilibrium equation is expressed by the following relation [18]:

$$\int_{\Omega} \boldsymbol{\sigma} \cdot \delta(\boldsymbol{\varepsilon}) dv - \int_{\Gamma} \mathbf{F} \cdot \delta \mathbf{u} ds = 0$$
 (14)

In the above relation, $\boldsymbol{\sigma}$, $\boldsymbol{\varepsilon}$, \mathbf{F} and \mathbf{u} are stress, strain, surface traction, and displacement vectors respectively. Γ is a part of domain boundary Ω on which traction \mathbf{F} is applied. For axisymmetric problems stress and strain vectors are as follows [16]:

$$\boldsymbol{\sigma} = [\sigma_r, \sigma_\theta, \sigma_z, \sigma_{rz}]^T, \quad \boldsymbol{\varepsilon} = [\varepsilon_r, \varepsilon_\theta, \varepsilon_z, \varepsilon_{rz}]^T$$
 (15)

Stress vector is expressed in terms of strain vector by means of Hook's law [16]:

$$\boldsymbol{\sigma} = \mathbf{D}\boldsymbol{\varepsilon}$$
 (16)

Matrix \mathbf{D} is defined in Ref. [16] for an orthotropic cylinder.

4 MESH-FREE NUMERICAL ANALYSIS

In this paper, moving least square (MLS) shape functions are used for approximation of displacement vector in the weak form of motion equation [23]. Displacement vector \mathbf{u} can be approximated by MLS shape functions as [16]:

$$\mathbf{u} = [u_r, u_z]^T = \boldsymbol{\Phi} \hat{\mathbf{u}}$$
 (17)

Where $\hat{\mathbf{u}}$ and $\boldsymbol{\Phi}$ are virtual nodal values vector and shape functions matrix respectively [16].

$$\hat{\mathbf{u}} = [(\hat{u}_r)_1, (\hat{u}_z)_1, \dots, (\hat{u}_r)_N, (\hat{u}_z)_N]^T$$
 (18)

$$\boldsymbol{\Phi} = \begin{bmatrix} \Phi_1 & 0 & \Phi_2 & 0 & \dots & \Phi_N & 0 \\ 0 & \Phi_1 & 0 & \Phi_2 & \dots & 0 & \Phi_N \end{bmatrix}$$
 (19)

N is the total number of nodes. By using Eq. (17) for approximation of displacement vector, strain vector can be expressed in terms of virtual nodal values:

$$\boldsymbol{\varepsilon} = \mathbf{B} \hat{\mathbf{u}}$$
 (20)

Matrix \mathbf{B} is defined in Ref. [16]. Substitution of Eqs. (16), (17) and (20) in Eq. (14) leads to:

$$\mathbf{k} \hat{\mathbf{u}} = \mathbf{f}$$
 (21)

Where

$$\mathbf{k} = \int_{\Omega} \mathbf{B}^T \mathbf{D} \mathbf{B} dv \quad \mathbf{f} = \int_{\Gamma} \Phi^T \mathbf{F} ds \quad (22)$$

For numerical integration, problem domain is discretized to a set of background cells with gauss points inside each cell. Then global stiffness matrix \mathbf{k} is obtained numerically by sweeping all gauss points inside Ω . Similarly global force vector \mathbf{f} is formed numerically in the same manner but by sweeping all gauss points on Γ . Imposition of essential boundary conditions in the system of Eq. (21) is not possible, because MLS shape functions don't satisfy the Kronecker delta property. In this work transformation method is used for imposition of essential boundary conditions. For this purpose transformation matrix is formed by establishing relation between nodal displacement vector \mathbf{U} and virtual displacement vector $\hat{\mathbf{u}}$ [16].

$$\mathbf{U} = \mathbf{T} \hat{\mathbf{u}} \quad (23)$$

\mathbf{T} is the transformation matrix and is defined in Ref. [16]. By using Eq. (23) system of linear Eq. (21) can be rearranged as:

$$\hat{\mathbf{k}} \mathbf{U} = \mathbf{f} \quad (24)$$

Where,

$$\hat{\mathbf{k}} = \mathbf{T}^{-T} \cdot \mathbf{k} \cdot \mathbf{T}^{-1} \quad , \quad \hat{\mathbf{f}} = \mathbf{T}^{-T} \cdot \mathbf{f} \quad (25)$$

Now the essential boundary conditions can be enforced to the modified equations system Eq. (24) easily like the finite element method.

5 RESULTS AND DISCUSSIONS

In this section, the proposed mesh-free method and the calculation model of the nanocomposite modulus are verified and then, effects of various parameters on the stress distribution of CNTRC cylinders are investigated. Fig. 2 shows a schematic drawing of a clamped-free cylinder under internal and external pressure in axisymmetric state.

5.1. Model Validation

At first, accuracies of the results are examined by comparing the results of isotropic FGM cylinders from mentioned Mesh-free method with FEM and the published results in previous works. Consider infinite length FGM cylinders subjected to internal pressure

(P_i , from inside to outside) with ratios of inner radius to outer radius (r_i/r_o) equal to 0.1 and 0.5. Variation of modulus of elasticity along the radius of the cylinder is as follows [24]:

$$E = E_i + \left(\frac{r^n - r_i^n}{r_o^n - r_i^n} \right) (E_o - E_i) \quad (26)$$

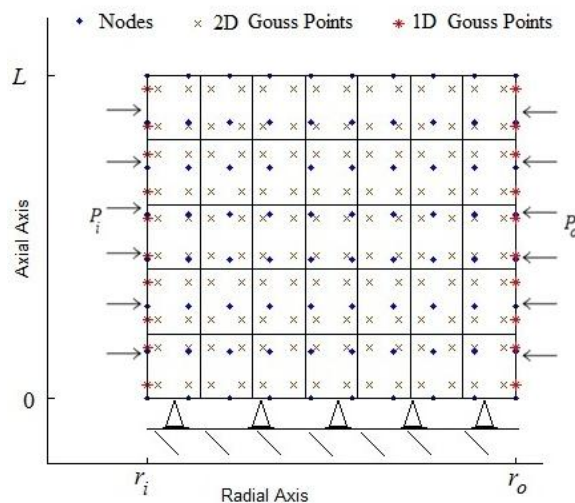
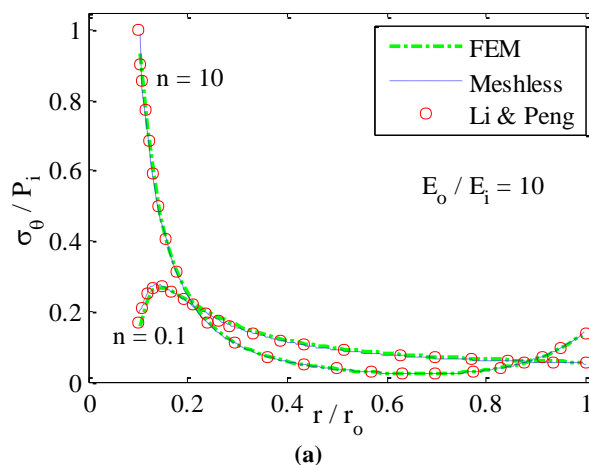


Fig. 2 Schematic sketch of an axisymmetric clamped-free cylinder subjected to internal and external pressure

In this analysis, ratio of modulus in the outer radius to the inner radius is considered to be $E_o/E_i = 10$, where the results for two different values of $n = 0.1, 10$ are presented. Results of mesh-free and finite element methods for the normalized hoop stress (σ_{θ}/P_i) are compared with the results reported by Li and Peng [24] where a very good agreement is observed between them (Fig. 3). In addition, comparison of these figures show the effect of volume fraction exponent and also the effect of cylinder thickness on the hoop stress distribution.



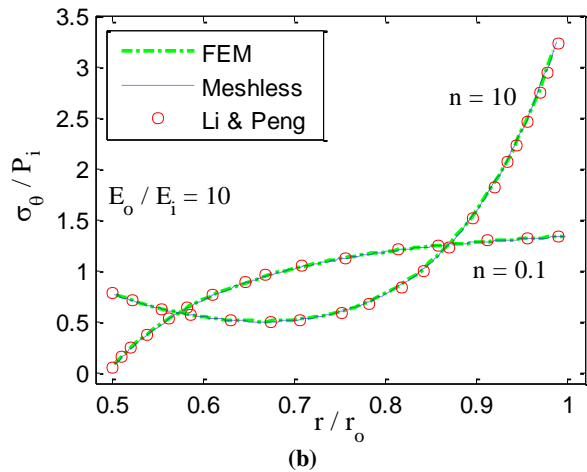


Fig. 3 Normalized hoop stress of FGM cylinders in radial direction for (a) $r_i/r_o = 0.1$, (b) $r_i/r_o = 0.5$.

Now, the calculation model of the nanocomposite modulus is examined, as Fig. 4 shows the calculations model of the nanocomposite modulus, E_1 , compared to experimental data from different literature sources. The model is able to be fitted to the experimental data in all cases investigated for very different aspect ratios CNTs. Our results are in agreement with the argument proposed by Martone et al. [14].

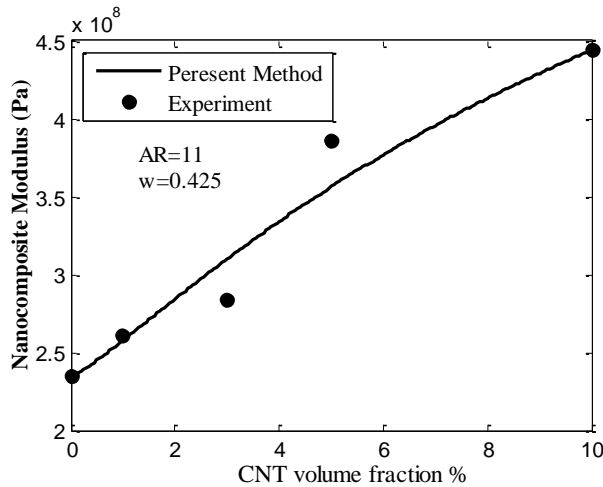


Fig. 4 Comparison of the Young's moduli of CNT-reinforced composite at different volume fraction of CNT with the experimental data [14].

5.2. CNTRC cylinders

After the validation of the proposed method, stress distribution in UD and FG-CNTRC cylinders are investigated by the proposed mesh-free method and FEM. In the following simulations CNTRC cylinders are considered to be made of Poly (methyl-methacrylate, referred as PMMA) as matrix, with CNT

as fibres aligned in the axial direction. PMMA is an isotropic material with $E^m = 2.5 \text{ GPa}$, $\nu^m = 0.34$ and $\rho^m = 1150 \text{ Kg/m}^3$. The (10,10) SWCNTs are selected as reinforcements. The material properties adopted for SWCNT are: $E_1^{CN} = 5.6466$, $E_2^{CN} = 7.0800$, $G_{12}^{CN} = 1.9445 \text{ TPa}$, $\rho^{CN} = 1400 \text{ Kg/m}^3$ and $\nu_{12}^{CN} = 0.175$ [11]. Han and Elliott [8] obtained the elastic moduli of polymer/CNT composite through MD simulation and energy minimization. In conventional rule-of-mixtures it is assumed that the whole system is continuum and that the interfaces between the matrix and filler material remain fully intact, therefore the general macroscopic rule of mixtures cannot be applied straightforwardly to composites with strong interfacial interactions. Also, micromechanics equations cannot capture the scale difference between the nano and micro levels. In order to overcome these lacks, CNT efficiency parameters, η_j ($j=1,2,3$) must be applied; therefore the material properties of CNTs become size-dependent.

By matching the young's moduli E_1^{CN} and E_2^{CN} of CNTRCs obtained by the extended rule of mixture to those by MD simulation, the CNT efficiency parameter can be calculated. It should be noticed that there are no MD result available for shear modulus G_{12} . Typical results are listed in Table 1 and will be used in all of the following examples, in which taking $\eta_3 = 0.7\eta_2$ [25]. It can be seen that there is a good agreement between the Young's moduli obtained from rule of mixture and MD simulation in Table 1, if η_1 and η_2 are properly chosen.

Table 1 Comparisons of young's moduli for polymer/CNT composites reinforced by (10,10) SWCNT at $T_0 = 300 \text{ K}$ [26].

V_{CN}^*	MD [8]		Extended Rule of mixture			
	E_{11} (GPa)	E_{22} (GPa)	E_{11} (GPa)	η_1	E_{22} (GPa)	η_2
0.12	94.6	2.9	94.78	0.137	2.9	1.022
0.17	138.9	4.9	138.68	0.142	4.9	1.626
0.28	224.2	5.5	224.50	0.141	5.5	1.585

At first, infinite length CNTRC cylinders are considered with CNT volume fraction, $V_{CN}^* = 0.17$, aspect ratio, $AR = 500$, and waviness index equal to, $w = 2$. In these cylinders, the ratio of inner radius to outer is equal to $r_i/r_o = 0.6$, subjected to internal pressure (P_i , from inside to outside). In the first analysis, the effect of CNT distribution on stress and displacement fields was examined.

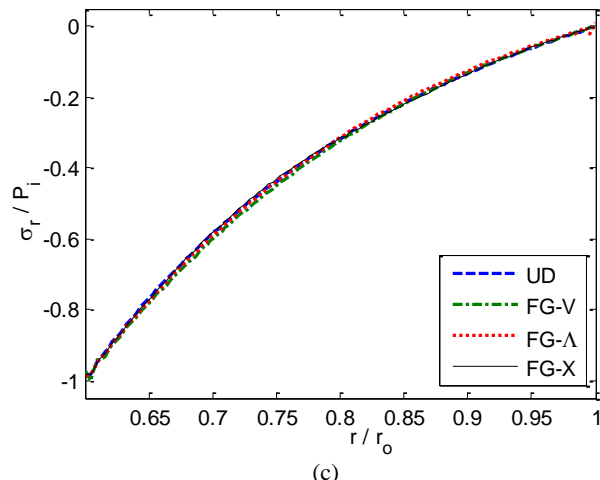
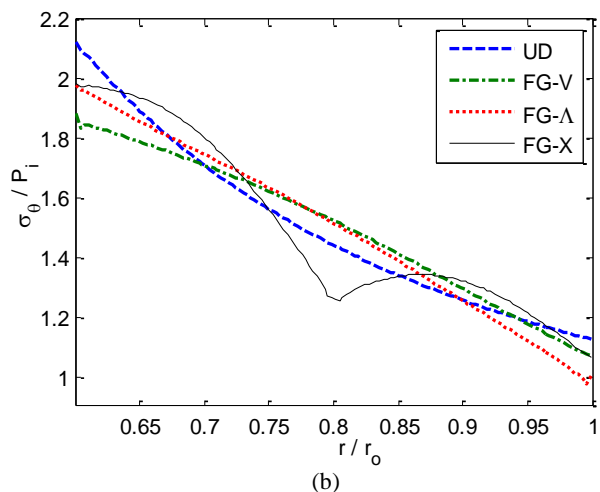
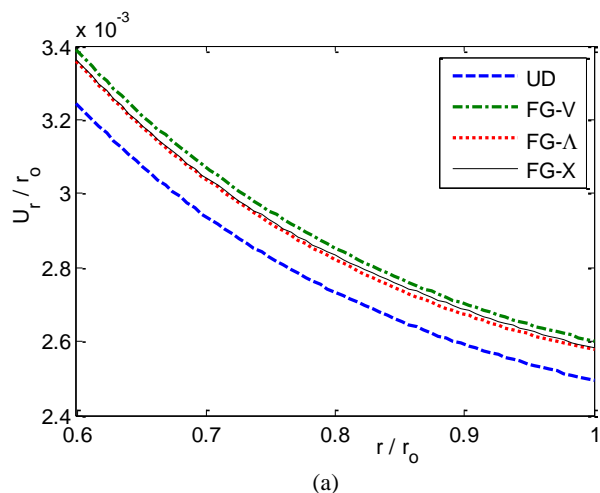


Fig. 5 Normalized (a) radial displacement (b) hoop stress (c) radial stress in radial direction for first model of CNTRC cylinders

Fig. 5 shows normalized displacement and stress distributions for an UD-CNTRC cylinder and three types of FG-CNTRC cylinders, i.e. FG-V, FG-Δ and

FG-X. These figures disclose that the radial displacement in FG-CNTRC cylinders are more than UD ones and FG-V type has the biggest values of radial displacement.

Although, in nanocomposite cylinders reinforced by straight CNT ($w = 0$), these values of UD-CNTRC were between corresponding values of FG-CNTRC [18]. Also, it can be seen, that CNT distribution has significant effect on hoop stress distribution, and their maximum and minimum values are accrued at inner and outer radius respectively. According to this figure, in FG-CNTRC cylinders, hoop stress has a considerable drop where volume fractions of CNTs become zero. The radial stress is uniformly varied from the value of internal pressure ($-P_i$) at inner surface to value of external pressure (zero) at outer surface.

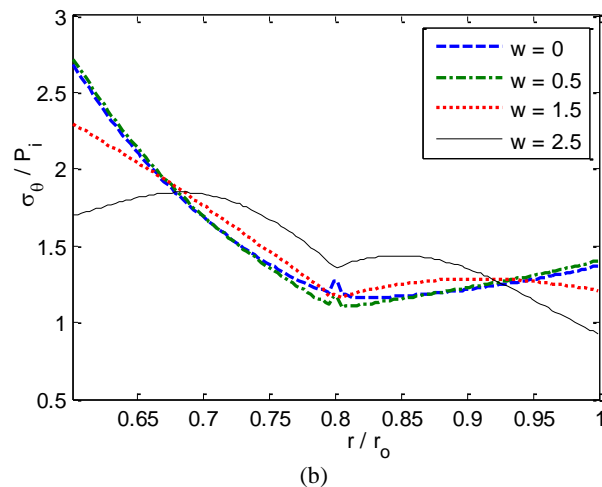
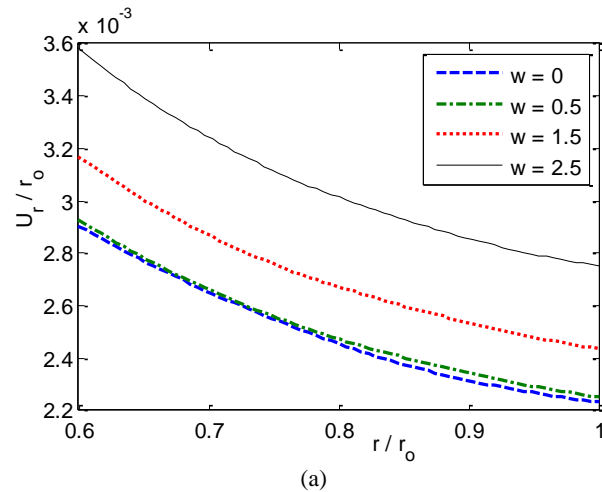


Fig. 6 Normalized (a) radial displacement (b) hoop stress in radial direction for second model of X-CNTRC cylinders

Second model is X-CNTRC cylinders similar to the first model with various values of waviness index ($w = 0, 0.5, 1.5, 2.5$), so the effect of CNT waviness is examined. Fig. 6 shows normalized radial displacement

and hoop stress of these X-CNTRC cylinders. These figures reveal that, increasing waviness index, especially for $w > 0.5$, has a significant effect on the static response of these cylinders and increases the values of radial displacement. Also, increasing CNT waviness decreases maximum values of hoop stress and even changes their location.

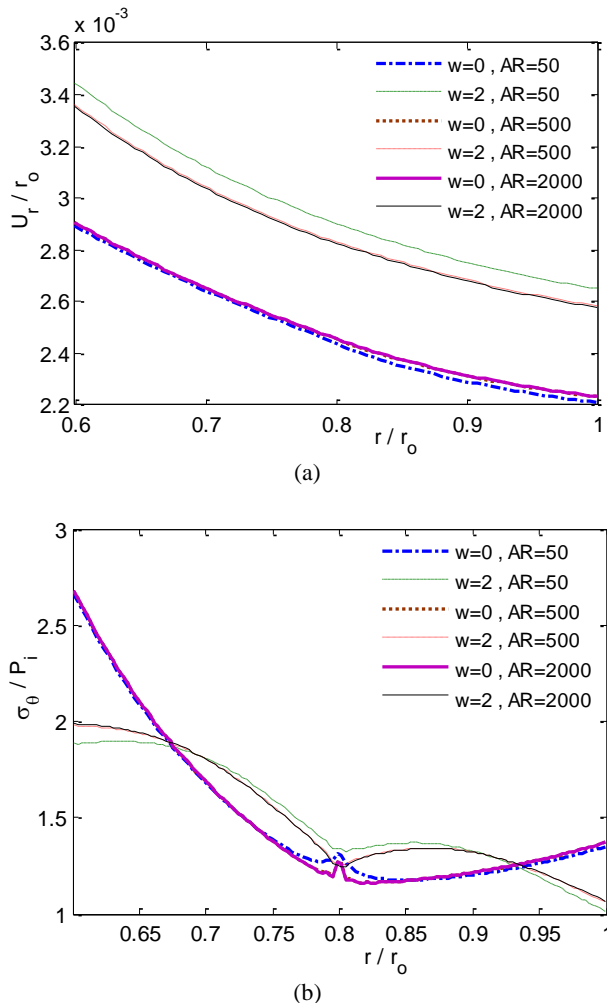


Fig. 7 Normalized (a) radial displacement (b) hoop stress in radial direction for third model of X-CNTRC cylinders

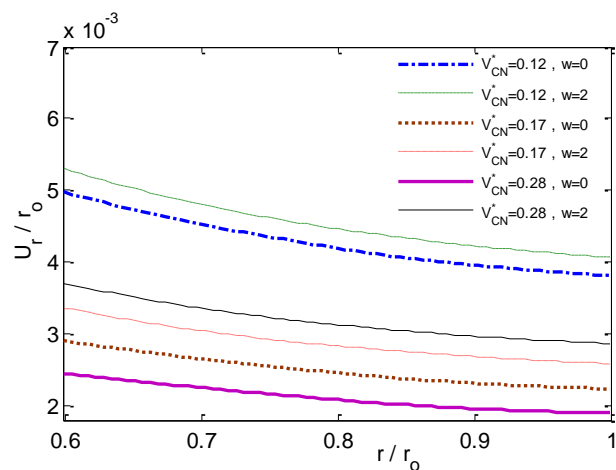
Regarding the third model, the effect of CNT aspect ratio is investigated for straight and wavy CNTRC cylinders, ($w = 0, 2$). This model is X-CNTRC cylinders with ratio of radii, $r_i/r_o = 0.6$, CNT volume fraction, $V_{CN}^* = 0.17$, and aspect ratio, $AR = 50, 500, 2000$. Fig. 7 shows normalized radial displacement and hoop stress of third model. It can be seen that CNT waviness index has more effect on the static response of CNTRC cylinders than CNT aspect ratio; value of aspect ratio has more considerable effect on wavy CNTRC than straight one. Fig. 7 shows increasing

CNT aspect ratio value, increases radial displacement values of straight CNTRC cylinders but decreases the corresponding values of wavy ones. Also, this increasing leads to increasing on hoop stresses of both types of CNTRC cylinders except around mid-radius. The effect of nanotube volume fraction is investigated by the forth model for straight and wavy CNTRC cylinders, ($w = 0, 2$). This model is X-CNTRC cylinders like as previous model with $AR = 500$ and various values of volume fraction of nanotube, $V_{CN}^* = 0.12, 0.17, 0.28$.

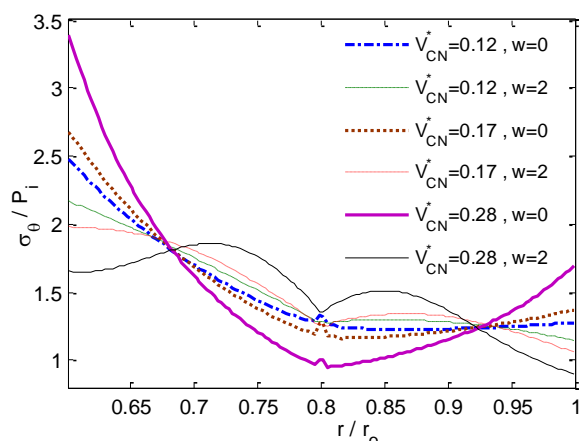
Fig. 8 illustrates static responses of this model under internal pressure like as the first model. These figures disclose increasing of CNT volume in straight nanotube ($w=0$) decreases radial displacement values, however, in cylinders with wavy nanotube, minimum values of displacement are observed for $V_{CN}^* = 0.17$. While, CNT volume has an attractive effect on hoop stress distribution. In cylinders with straight CNT, increasing nanotube volume increases maximum values of hoop stress and also decreases its minimum value as well. While in cylinders with wavy nanotubes, locations of maximum/minimum values change by CNT volume increasing.

It can be seen that increasing CNT volume increases differences between radial stress values of these cylinders with straight and wavy nanotube. In fifth model, the effect of CNTRC cylinder thickness is investigated. In this model, CNTRC cylinders are considered like as the first model with ratio of radii equal to, $r_i/r_o = 0.9$. Fig. 9 shows normalized radial displacement and hoop stress of these cylinders. Comparing between Fig. 5 and Fig. 9, shows that decreasing CNTRC cylinder thickness may lead to an increase in the radial displacement and hoop stress. Also, this reduction changes the locations and values of maximum and minimum hoop stress especially for FG-CNTRC cylinders.

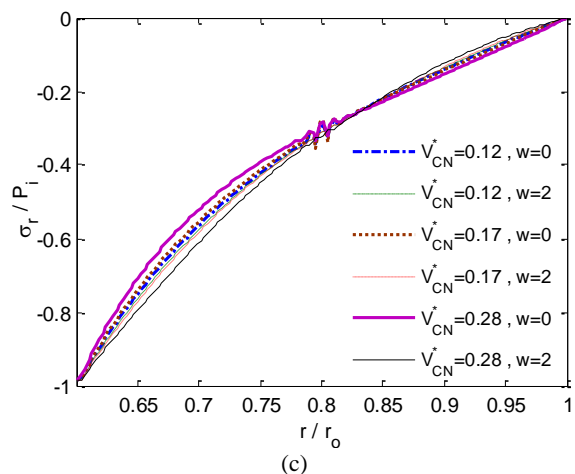
All of the previous models were having infinite length (plane strain) cylinders. Now, consider a clamed-free X-CNTRC cylinder with ratio of length to outer radius, $L/r_o = 3$, ratio of radii, $r_i/r_o = 0.8$, CNT volume fraction, $V_{CN}^* = 0.17$, aspect ratio, $AR = 500$, and waviness index equal to, $w = 2$, that is subjected to internal and external pressure ($P_o = 0.5P_i$) like as Fig. 2. Von-mises stress, radial stress, hoop stress, axial stress and also radial and axial displacement distributions are shown in Fig. 10. There are some disturbances around $z=0$ in stress distributions because of the boundary condition and drops around mid-radius of cylinder because CNT volume becomes zero. It can be seen that maximum displacement and von-mises stress are examined at $z = L$ of inner surface.



(a)

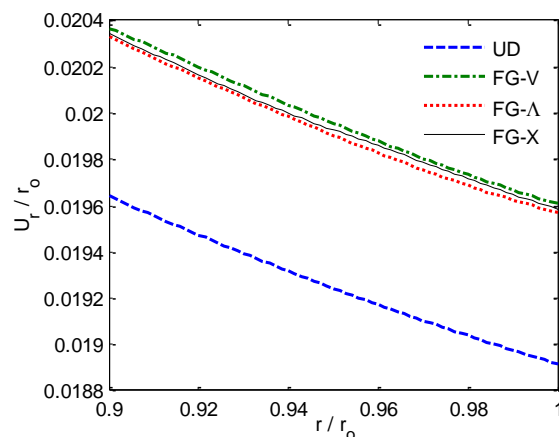


(b)

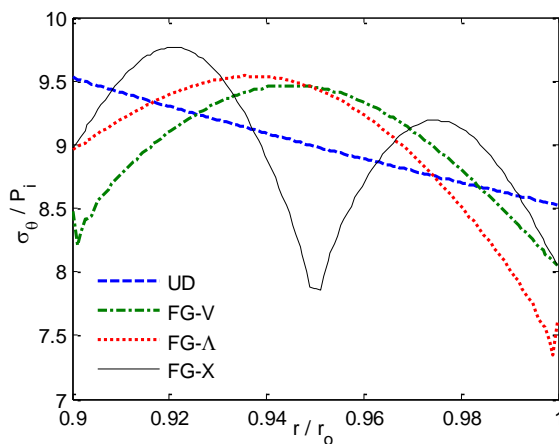


(c)

Fig. 8 Normalized (a) radial displacement (b) hoop stress (c) radial stress in radial direction for fourth model of X-CNTRC cylinders



(a)



(b)

Fig. 9 Normalized (a) radial displacement (b) hoop stress in radial direction for fifth model of CNTRC cylinders.

6 CONCLUSION

The effects of CNTs aspect ratio and waviness index are analyzed on the stress and displacement distributions of functionally graded nanocomposite cylinders reinforced by wavy carbon nanotube based on developed mesh-free method. The material properties of CNTRC are assumed to be graded in the radius and estimated through new version of Rule of mixture. CNT waviness plays a critical role for distributions and values of stress and displacement in CNTRC cylinders. The effects of aspect ratio, volume and distribution kind of wavy CNTs and geometry dimensions on the static behavior of FG-CNTRC cylinders were discussed in detail and the following results were obtained from this analysis:

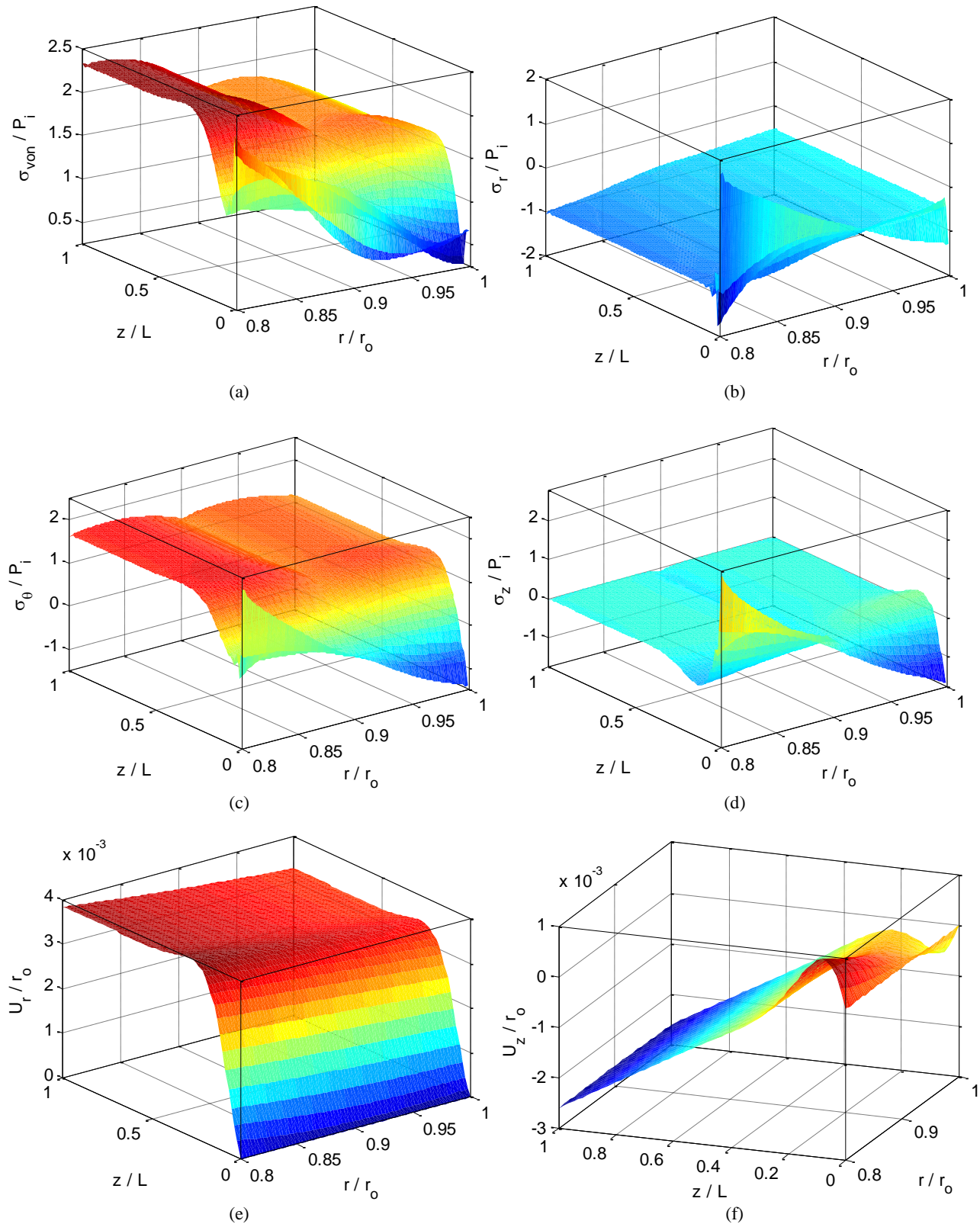


Fig. 10 Normalized (a) von-mises stress (b) radial stress (c) hoop stress (d) axial stress (e) radial displacement (f) axial displacement in radial direction for the finite length X-CNTRC cylinder.

- For $w = 2$, radial displacement values of FG-CNTRC cylinders are more than UD ones but for cylinders reinforced by straight CNT, these values of UD-CNTRC are between corresponding values of FG-CNTRC.
- Increasing waviness index increases the values of radial displacement but decreases maximum values of hoop stress and even changes their location.
- Increasing CNT aspect ratio and volume fraction have different effects on the static responses of cylinders reinforced by straight and wavy CNT.
- CNT waviness has more effect on the static response of CNTRC cylinders than CNT aspect ratio and also, value of aspect ratio has more considerable effect on wavy CNTRC than straight one.
- Decreasing CNTRC cylinder thickness may lead to an increase in the values of radial displacement and hoop stress and also changes the locations and values of maximum and minimum hoop stress.

REFERENCES

- [1] Iijima, S., "Helical microtubules of graphitic carbon", *Nature*, Vol. 354, 1991, pp. 56-8.
- [2] Zhu, R., Pan, E., and Roy, A. K., "Molecular dynamics study of the stress-strain behavior of carbon-nanotube reinforced Epon 862 composites", *Materials Science and Engineering A*, Vol. 447, 2007, pp. 51-7
- [3] Machado, M. A. L., Valentini, L., Biagiotti, J., and Kenny, J. M., "Thermal and mechanical properties of single-walled carbon nanotubes-polypropylene composites prepared by melt processing", *Carbon*, Vol. 43, 2005, pp. 1499-505.
- [4] Qian D., Dickey E. C., Andrews R., and Rantell T., "Load transfer and deformation mechanisms in carbon nanotube-polystyrene composites", *Applied Physics Letters*, Vol. 76, 2000, pp. 2868-70.
- [5] Mokashi, V. V., Qian, D., and Liu, Y. J., "A study on the tensile response and fracture in carbon nanotube-based composites using molecular mechanics", *Composites Science and Technology*, Vol. 67, 2007, pp. 530-40.
- [6] Gojny, F. H., Wichmann, M. H. G., Fiedler, B., and Schulte, K., "Influence of different carbon nanotubes on the mechanical properties of epoxy matrix composites – A comparative study", *Composites Science and Technology*, Vol. 65, 2005, pp. 2300-13.
- [7] Fidelus, J. D., Wiesel, E., Gojny F. H., Schulte, K., and Wagner H. D., "Thermo-mechanical properties of randomly oriented carbon/epoxy nanocomposites", *Composite Part A* Vol. 36, 2007, pp. 1555-61.
- [8] Han, Y., Elliott, J., "Molecular dynamics simulations of the elastic properties of polymer/carbon nanotube composites", *Computational Materials Science*, Vol. 39, 2007, pp. 315-23.
- [9] Coto B., Antia I., Blanco M., Martinez-de-Arenaza I., Meaurio E., Barriga J., et al., "Molecular dynamics study of the influence of functionalization on the elastic properties of single and multiwall carbon nanotubes", *Computational Materials Science*, Vol. 50, 2011, pp. 3417-24.
- [10] Shen H. S., "Nonlinear bending of functionally graded carbon nanotube reinforced composite plates in thermal environments", *Composite Structures*, Vol. 91, 2009, pp. 9-19.
- [11] Shen H. S., "Postbuckling of nanotube-reinforced composite cylindrical shells in thermal environments, Part I: Axially-loaded shells", *Composite Structures*, Vol. 93, 2011, pp. 2096-108.
- [12] Shen H. S., Xiang Y., "Nonlinear vibration of nanotube-reinforced composite cylindrical shells in thermal environments", *Computer Methods in Applied Mechanics and Engineering*, Vol. 213, 2012, pp. 196-205.
- [13] Montazeri, A., Javadpour, J., Khavandi, A., Tcharkhtchi, A., and Mohajeri, A., "Mechanical properties of multi-walled carbon nanotube/epoxy composites", *Materials and Design*, Vol. 31, 2010, pp. 4202-8.
- [14] Martone, Faiella, G., Antonucci, V., Giordano, M., and Zarrelli M., "The effect of the aspect ratio of carbon nanotubes on their effective reinforcement modulus in an epoxy matrix", *Composites Science and Technology*, Vol. 71, 2011, pp. 1117-23.
- [15] Jam, J. E., Pourasghar, A., kamarian, S., "The effect of the aspect ratio and waviness of CNTs on the vibrational behavior of functionally graded nanocomposite cylindrical panels", *Polymer Composite*, Vol. 33, 2012, pp. 2036-44.
- [16] Moradi-Dastjerdi, R., Pourasghar, A., Foroutan, M., and Bidram, M., "Vibration analysis of functionally graded nanocomposite cylinders reinforced by wavy carbon nanotube based on mesh-free method", *Journal of Composite Materials*, Vol. 48, 2014, pp. 1901-13.
- [17] Moradi-Dastjerdi, R., Foroutan, M., and Pourasghar, A., "Dynamic analysis of functionally graded nanocomposite cylinders reinforced by carbon nanotube by a mesh-free method", *Materials and Design*, Vol. 44, 2013, pp. 256-66.
- [18] Moradi-Dastjerdi, R., Foroutan, M., Pourasghar, A., and Sotoudeh-Bahreini R., "Static analysis of functionally graded carbon nanotube-reinforced composite cylinders by a mesh-free method", *Journal of Reinforced Plastic and Composites*, Vol. 32, 2013, pp. 593-601.
- [19] Ghayoumizadeh H., Shahabian F., and Hosseini S. M., "Elastic wave propagation in a functionally graded nanocomposite reinforced by carbon nanotubes employing meshless local integral equations (LIEs)", *Engineering Analysis with Boundary Elements*, Vol. 37, 2013, pp. 1524-31.
- [20] Foroutan, M., Moradi-Dastjerdi, R., and Sotoodeh-Bahreini R., "Static analysis of FGM cylinders by a mesh-free method", *Steel and Composite Structures*, Vol. 12, 2012, 1-12.
- [21] Mollarazi, H. R., Foroutan, M., and Moradi-Dastjerdi, R., "Analysis of free vibration of functionally graded material (FGM) cylinders by a meshless method", *Journal of Composite Materials*, Vol. 46, 2011, 507-15.

- [22] Foroutan, M., Moradi-Dastjerdi, R., “Dynamic analysis of functionally graded material cylinders under an impact load by a mesh-free method”, *Acta Mechanica*, Vol. 219, 2011, pp. 281-90.
- [23] Lancaster, P., Salkauskas, K., “Surface Generated by Moving Least Squares Methods”, *Mathematics of Computation*, Vol. 37, 1981, pp. 141-58.
- [24] Li, X. F., Peng, X. L., “A pressurized functionally graded hollow cylinder with arbitrarily varying material properties”, *Journal Elasticity*, Vol. 96, 2009, pp. 81-95.
- [25] Song, Y. S., Youn, J. R., “Modeling of effective elastic properties for polymer based carbon nanotube composites”, *Polymer*, Vol. 47, 2006, pp. 1741-8.
- [26] Shen, H. S., Zhang, C. L., “Thermal buckling and postbuckling behavior of functionally graded carbon nanotube-reinforced composite plates”, *Materials and Design*, Vol. 31, 2010, pp. 3403-11.